Medium frequency transformer in resonant switching dc/dc-converters for railway applications

Holger Hoffmann, Bernhard Piepenbreier
University of Erlangen-Nuremberg - Chair of Electrical Drives and Machines
Cauerstr. 9
91058 Erlangen, Germany
Phone: +49 (0) 9131-8527790
Fax: +49 (0) 9131-8527658
Email: hoffmann@eam.eei.uni-erlangen.de
URL: http://www.eas.e-technik.uni-erlangen.de/

Keywords

Soft switching, ZCZVS converters, High voltage power converters, Transformer, Cooling

Abstract

A converter system based on medium frequency dc/dc-converters can replace the conventional traction transformer saving both mass and energy.
A medium-frequency-transformer design-procedure is introduced that allows a clear representation of transformers total mass and efficiency under consideration of thermal aspects. Measurements with a prototyped mf-transformer verify the calculated results.

Introduction

Contemporary railway power supplies for AC-mains contain a line-transformer in the propulsion chain. Especially for the 16.7 Hz main lines this transformers are heavy (about 9.3t for ICE 3), expensive, have a low efficiency of about 92% and take too much of the narrow space in passenger vehicles with under floor housing of the drive power chain. Especially double deck trains can be a challenge.

Weight reduction and an increase of efficiency of the transformers is therefore a matter of priority for the next generation of modern AC-fed traction vehicles.
To avoid the disadvantages several solutions have been proposed [1, 2, 3] that utilize transformers operating at frequencies well above the line frequency.

In the analyzed concept series-connected converter submodules on different electrical potential are linked to a common dc-link by isolating dc/dc converters. The isolating transformers operate at medium frequency (mf).

As shown in [4] the chosen semiconductors, the switching frequency, the type of switching and chosen transformer core and transformer conductor materials have significant impact on the total system costs, the total efficiency and mass reduction.

This paper deals with the potential efficiency and mass of the mf-transformer inside the dc/dc converters. A transformer topology is introduced and discussed concerning the resulting transformer efficieny and transformer mass by variation of core- and conductor materials as well as cooling- and isolation-concepts under consideration of thermal aspects.

Furthermore the experimental results of a prototyped mf-transformer, built up with direct hollow conductor cooling are shown in order to verify the calculated conductor losses, core losses and thermal parameters.

1 Resonant switching dc/dc converter

The investigated topology is based on series-connected converter submodules at the line side. Each converter submodule consists of a four Quadrant Converter (4QC) and a mf dc/dc-converter as key component, including the mf-transformer. Its operating frequency is much higher than the line frequency, thus mass and size is lower.

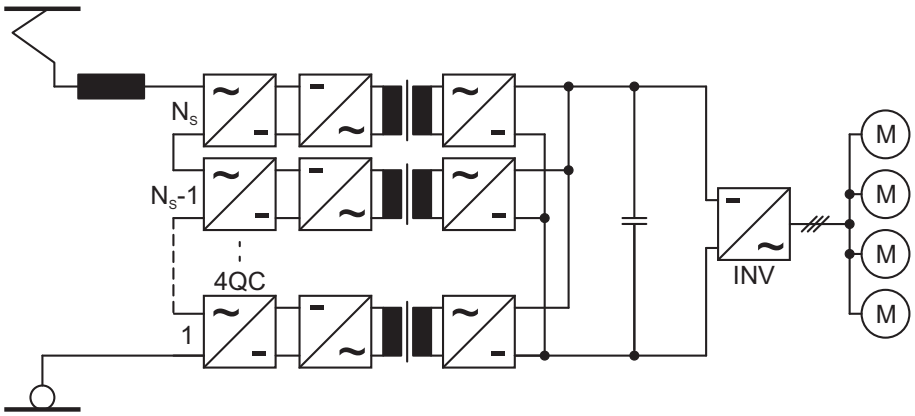

Figure 1: Railway power supply with single-phase 4-Quadrant-Converters (4QC) and mf dc/dc-converters

Fig. 1 shows the analyzed topology. The number N_S of single converter cells depends on the maximum line voltage $U_{L\,max}$, the DC link voltage U_{dc} and the voltage margin U_{mrg} to control the line current as well as the level of redundancy k_{red}.

The last parameter defines the number of series-connected converter cells that can fail without having any negative impact on the system availability.

The affordable number of stages N_S can be calculated as follows:

$$N_S - k_{red} = \frac{\sqrt{2} \cdot U_{L\,max} + U_{mrg}}{U_{dc}} \tag{1}$$

The higher the chosen DC link voltage, the lower the number of converter cells to be cascaded serially. Fig. 2 shows the correlation for a voltage margin $U_{mrg} = 10\%\ U_{L\,max}$.

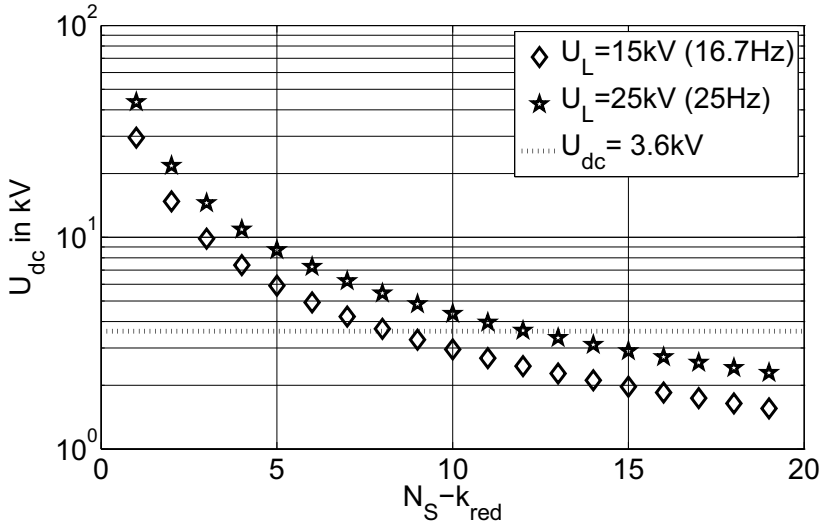

Figure 2: Number of stages N_S as a function of maximum line voltage $U_{L\,max}$, dc-link voltage U_{dc} and the reserved voltage margin U_{mrg}

The afterwards shown results of mf-transformer calculations apply to calculations based on a line voltage of 25 kV. The affordable number of stages is $N_S \geq 12$, where 12 is true without any redundancy (see in Fig. 2).

2 Design of mf-transformer

In addition to the mf-transformers switching frequency [4] both the transformer design and chosen conductor-, core- and insulation-material play a major role concerning the resulting transformer efficiency and mass.

An analytic comparison of different core- and conductor materials, under consideration of thermal aspects, has shown, that the optimum compromise between transformer efficiency and transformer mass results for a transformer with internal cooled conductors. The afterwards shown transformer optimization is performed concerning the aforementioned design. For comparison nanocrystalline, amorphous and ferrite core material is used.

The isolation between primary and secondary winding is realized by oil and between adjacent conductors inside one layer by an isolation material such as NOMEX. The conductors are designed as hollow profile type in aluminium (wall thickness = skin depth). Conductor cooling is provided by deionized water flow through the aluminium profiles.

In that case the net-transformer mass is mostly defined by the core. Under consideration of a certain dc/dc-converter switching frequency (here 5.6 *kHz*), fixed isolation gaps and a given degree of interleaving both winding number and current density (depends on conductor dimensions [4]) have significant impact on the resulting transformer mass. In order to find a combined optimum of mass and efficiency a scope of winding numbers has to be determined that conform to the thermal requirements.

The lower boundary is defined by the maximum core hotspot temperature T_{HS} inside the core. In case of natural convection it can be described with a one dimensional model as a function of the outer edge lenght of the core d_k (quadratic cross-section), the volume specific core losses p_{vc}, the ambient temperatur T_A, the heat transfer coefficient α at the surface of the core and the thermal conductivity λ inside the core.

The afterwards shown derivation for determination of the core hotspot temperature T_{HS} is based on the geometry shown in Figure 3.

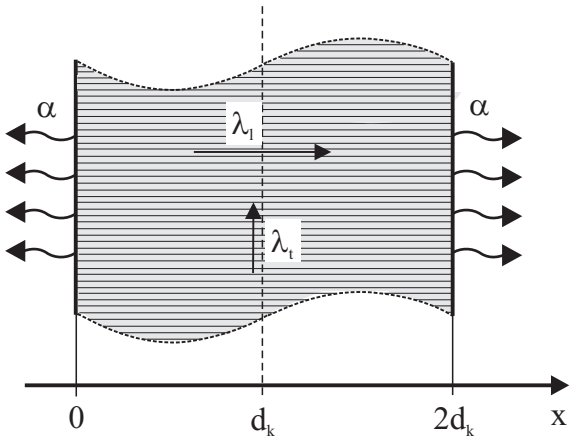

Figure 3: Geometry of 1-dimensional thermal model of the core for determination of hotspot temperatur T_{HS}

In case of tape wound cores like nanocrystalline VITROPERM 500F or amorphous VITROVAC 6030F it is assumed, that the main heat flux inside the core takes place inside the metal tapes. Therefore, the thermal conductivity in longitudinal direction of the layer plane λ_l is assumed to be significantly higher compared with the thermal conductivity λ_t in transverse direction. Hence, as shown in Fiugure 3, only two side surfaces participate in heat exchange with the enviroment.

This procedure may not be applied in case of ferrit cores. Due to the homogeneity of the core material an omnidirectional thermal conductivity ($\lambda_l = \lambda_q$) exists. In that case all core walls equally contribute to heat exchange with the enviromental coolant. The afterwards shown calculation can even be used for ferrit cores with a square cross sectional area. For this the removable specific heat quantity has to be doubled or the resulting maximum core temperature halved, compared with tape wound cores.

For a given maximum temperatur of surrounding coolant T_A (in case of natural convection at the top of the core) the maximum core hotspot temperatur T_{HS} in the centre of the analysed core for $x = d_k$ can be determined as follows. For use with ferrite cores the resulting core hotspot temperature has to be halved as mentioned above.

$$T_{HS}(x = d_k) = T_W + \int_0^{d_k} \frac{p_{vc} \cdot x}{\lambda} dx \tag{2}$$

$$T_W = T_A + \frac{p_{vc} \cdot d_k}{\alpha} \tag{3}$$

$$T_{HS} = T_A + p_{vc} \cdot d_k \left(\frac{1}{\alpha} + \frac{d_k}{2 \cdot \lambda} \right) \tag{4}$$

With the above shown formulas, curves can be plotted, that describe the resulting hotspot temperatur as a function of winding number for a given switching frequency and a given flux density inside the core. From this a minimum winding number can be selected that guarantees a compliance with the material specific maximum core temperature.

The upper boundary of the the scope of winding numbers that conforms to the thermal requirements is determined by the maximum water flow rate $\dot{V}_{water}$ inside the hollow conductor cooling system. It depends on the conductor losses P_{cond}, the volume-specific heat-capacity c_v, the density ρ and the maximum temperature difference ΔT of coolant.

$$\dot{V}_{water}(N_{max}, J) = \frac{P_{cond}(N_{max}, J)}{c_v \cdot \rho \cdot \Delta T} \tag{5}$$

The conductor losses in transformer windings essentially depend on chosen switching frequency (resulting skin depth), the conductor material (material-specific conductivity), the total winding lenght (depends on winding number and core diameter), the chosen degree of interleaving, the number of layers inside the winding and the resulting current density inside the hollow conductors. Several calculation schemes exist [8,9], that allow a calculation of conductor losses under consideration of the aformentioned parameters.

In order to analyse the influence of chosen current density on the resulting transformer-efficiency and -mass the current density has been varied under consideration of an identical wall thickness and an identical RMS current inside the conductors (results for given transferred power and given interlocking time).

As a result of proximity effect, the current flows predominantly in one wall of the aluminium hollow conductors. So a variation of current density leads to a variation of vertical conductor dimension. That means, that a higher current density results in lower vertical winding dimensions and even lower core dimensions but higher winding losses.

In the afterwards shown results the horizontal dimension of the hollow conductors have been chosen equal to 5mm.

Within the thermal limitations calculated by (4) and (5) the total losses and total transformer mass can be determined as a function of winding number N and current density J.

Fig. 4 and Fig. 5 show the achievable transformer efficiency, the transformer mass and the limiting values of winding number N_{min} and N_{max} for $T_{HS} = 120\ ^\circ C$ and $\dot{V}_{water} = 2\ l/min$ at a transferred power of 450 kW.

It is obvious, that both mass and efficiency significantly depend on chosen current density J. A decrease of current density (at a given winding number N) leads to an increase of transformer mass because of larger winding-window and consequently core-dimensions but higher efficiency due to lower conductor losses. A variation of winding number N has impact on both core cross-section-area, vertical core dimensions and winding lenght (conductor losses).

For small winding numbers (here $N \leq 18$) the total losses are mainly determined by the core due to its large cross section. In that range an increase of winding number leads to strong rise of efficiency and decrease of mass. The winding number at maximum efficiency primarily depends on the current density J (here $8 \leq N \leq 18$). For higher winding numbers the efficiency decreases because the total losses are increasingly determined by the winding losses due to a longer winding.

By use of this procedure with shown diagrams an optimum design, under consideration of application-specific requirements, can easily be selected.

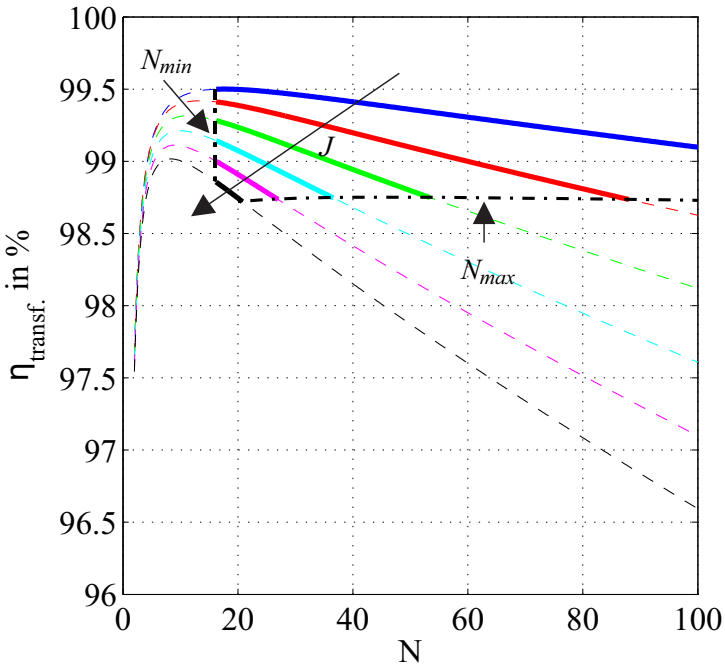

Figure 4: Transformer efficiency $\eta_{transf.}$ as a function of current density J and winding number N with limiting values of winding number N_{max} and N_{min} - nanocrystalline core material

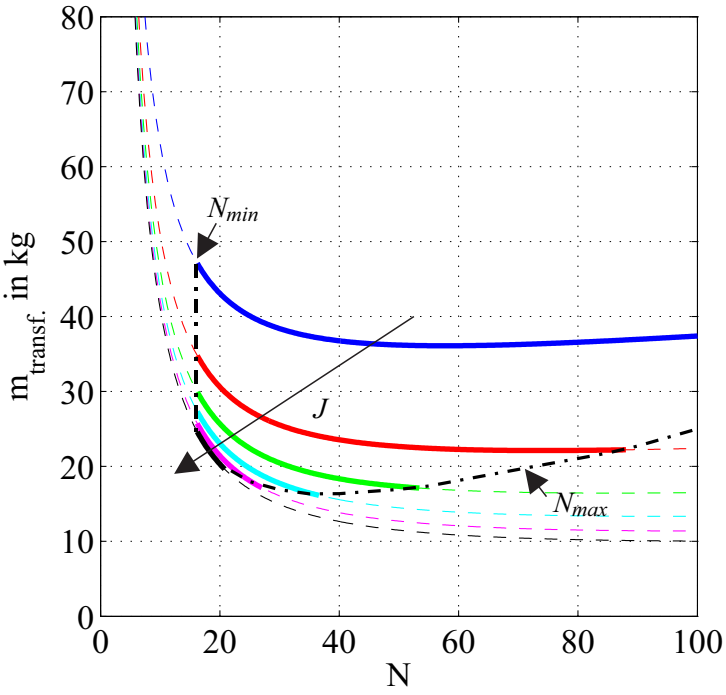

Figure 5: Transformer mass $m_{transf.}$ as a function of current density J and winding number N with limiting values of winding number N_{max} and N_{min} - nanocrystalline core material

Table 1 shows the extrema concerning the analyzed case under consideration of thermal aspects (maximum core- and maximum water-temperatures) at the example of nanocrystalline VITROPERM 500F.

Moreover a combined optimum can be selected between these limits that guarantees a compromise between efficiency and mass.

Table I: working points at maximum efficiency and minimum mass

	N	$\eta_{transf.}$ in %	$m_{transf.}$ in kg
Maximum $\eta_{transf.}$	18	99.5	47
Minimum $m_{transf.}$	36	98.75	16.5

In order to analyse further core materials the preset parameters for the electromagnetic calculation such as loss curves, maximum core hotspot temperatur and saturation flux density can be varied.

Thus, a comparison of different core materials can be established for identical thermal requirements. Table 2 shows the results of calculations for nanocrystalline VITROPERM 500F, amorphous VITROVAC 6030F and for ferrite K 2006.

The comparison is based on identical total transformer losses or identical transformer efficiency.
In order to analyse the influence of transformer efficiency on transformer mass the comparison is done at efficiencies of 98 % and 99 %.

Table II: Comparison of different core materials for transformer with internal cooled aluminium conductors

	VITROPERM 500F	VITROVAC 6030F	Ferrite K 2006
$\eta_{transf.} = 99\,\%$	38.1 kg	62.8 kg	n.p.
$\eta_{transf.} = 98\,\%$	24 kg	35.3 kg	142.6 kg

Table 2 shows, that the minimum transformer mass results, independent of chosen transformer efficiency, for the nanocrystalline core material. By use of amorphous material a higher transformer mass or lower efficiency at identical transformer mass results compared with nanocrystalline VITROPERM due to a lower saturation flux density and higher mass specific core losses.

The highest transformer mass results for the analysed ferrite material. A low saturation flux density in that case results in high core dimensions and thus in high transformer losses. So the transformer efficiency of 99 % cannot be reached by use of the analysed conductor material and conductor type.

3 Experimental results with prototyped mf-transformer

In order to verify the calculated values of transformer core- and conductor losses a mf-transformer has been prototyped. It was designed with interleaved windings. The degree of interleaving is chosen to 2 (2 primary and 2 secondary winding sections), which guarantees a suitable balance between core-mass, total conductor length and leakage inductance.

In order to reduce winding length a U-core type has been chosen instead of a central coloumn type core. The coils are placed on both legs. On each leg is, according to the chosen degree of interleaving, both primary and secondary winding.

Heat removal of conductors is provided by deionized water flow through the aluminium profiles and core-cooling by natural convection in oil.

The isolation between primary, secondary winding and the core is realized by oil. The isolation between adjacent conductors inside the winding is realized by an isolation material such as NOMEX.

The isolation distance between primary and secondary winding is chosen for a 25 kV line voltage. The isolation thickness between adjacent conductors inside the layers results for a defined isolation-material from the maximum dc-link voltage $U_{dc\,max}$, the dc/dc-converter-topology (half-/fullbridge) and the chosen winding number N. For a halfbridge-topology the isolation-voltage U_{iso} between adjacent conductors can be determined as follows:

$$U_{iso} = \frac{U_{dc\,max}}{2 \cdot N} \tag{6}$$

Fig. 6 shows both the geometrical shape of the analyzed mf-transformer and measurement results of core- [6,7] and conductor losses [8,9]. They have been characterized at rectangular voltage in test setups which permit realistic conditions.

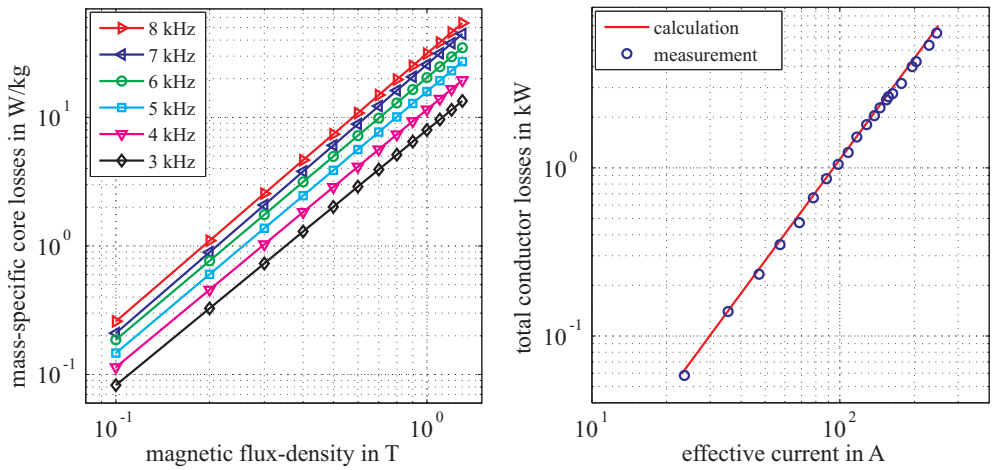

(a) mass-specific core losses p_m (b) conductor losses at 5.6 kHz

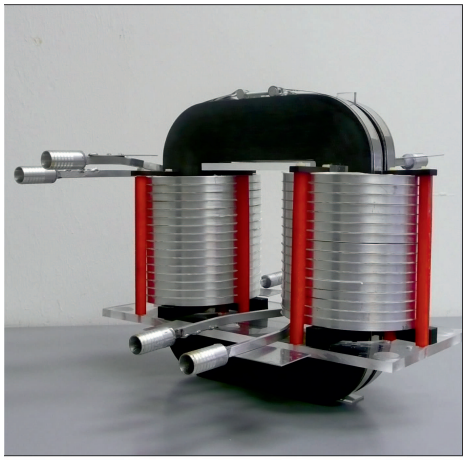

(c) prototyped mf-transformer

Figure 6: Experimental results with prototyped mf-transformer

4 Conclusion

One basic advantage of mf-dc/dc-converter technology is increased efficiency and reduced total mass when compared to conventional traction power supply. The mf-transformer as key-component plays an important role concerning the aforementioned parameters. A transformer with direct cooled hollow conductors was chosen in order to introduce a procedure that allows an application-specific design of mf-transformer under consideration of thermal aspects.

A coupled thermal, hydraulic and electromagnetic analysis of a transformer with internal liquid cooled conductors shows that nanocrystalline material has to be chosen for use in the mf-transformer in the favourable frequency range in order to reach minimum transformer mass and minimum transformer volume at maximum transformer efficiency.

To verify the applied models for conductor cooling, simplified tests with liquid cooled hollow conductor profiles have been carried out. But in order to get an exact description of cooling performance, core losses and conductor losses, under consideration of skin- and proximity-effects, measurements at a transformer prototype are inevitable.

Therefore, a prototype was developed that allowed measurements under realistic conditions in a dc/dc converter test setup. Experimental results with the prototyped mf-transformer showed very good accordance with the performed calculations

References

[1] Zuber D.; Mittelfrequente resonante DC/DC-Wandler fuer Traktionsanwendungen; Phd Zuerich 2001

[2] Diekerhoff S., Bernet S., Krug D. ; Power Loss-Oriented Evaluation of High Voltage IGBTs and Multilevel Converters in Transformerless Traction Applications; IEEE Transactions on power electronics, Vol. 20, No. 6, November 2005

[3] M. Steiner; Seriengeschaltete Gleichspannungszwischenkreisumrichter in Traktionsanwendungen am Wechselspannungsfahrdraht, Phd Zuerich 2000

[4] Hoffmann H., Piepenbreier B.; High Voltage IGBTs and Medium Frequency Transformer in DC-DC Converters for Railway Applications; SPEEDAM 2010, Pisa, Italy

[5] Weigel J., Nagel A., Hoffmann H.; High Voltage IGBTs in Medium Frequency Traction Power Supply; EPE 2009, Barcelona, Spain

[6] Han Y., Eberle W., Y. F. Liu; New Measurement Methods to Characterize Transformer Core Loss and Copper Loss in High Frequency Switching Mode Power Supplies; 35th Annual IEEE Power Electronics Specialists Conference, 2004

[7] Duerbaum, Th. and Albach M.; Core Losses in Transformers with an Arbitrary Shape of the Magnetizing Current; EPE Roc., Vol. 1, p. 1.171-1.176, Sevilla (Spain), 1995.

[8] P. L. Dowell; Effects of Eddy Currents in Transformer Windings, Proceedings IEE (UK), Vol. 113, No.8, August, 1966, pp. 1387-1394.

[9] L. Schuelting; Optimierte Auslegung induktiver Bauelemente fr den Mittelfrequenzbereich; Dissertation RWTH Aachen, 1993